Title
LOSS OF COHERENCY IN SPINODALLY DECOMPOSED Cu-Ni-Fe ALLOYS

Authors
Livak, R.J.
Thomas, G.

Publication Date
1973-07-01

Submitted to
Acta Metallurgica

LBL-1842
Preprint C.1

LOSS OF COHERENCY IN SPINODALLY DECOMPOSED Cu-Ni-Fe ALLOYS

R. J. Livak and G. Thomas

July 1973

Prepared for the U. S. Atomic Energy Commission
under Contract W-7405-ENG-48

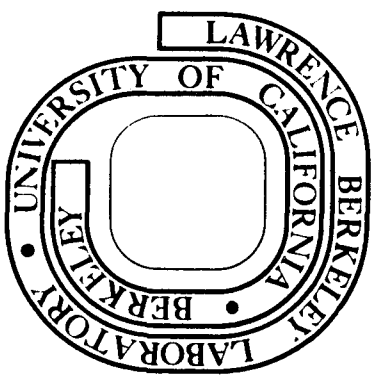

LBL-1842

DISCLAIMER

LOSS OF COHERENCY IN SPINODALLY DECOMPOSED Cu-Ni-Fe ALLOYS

R. J. Livak* and G. Thomas

Inorganic Materials Research Division, Lawrence Berkeley Laboratory and Department of Materials Science and Engineering, College of Engineering; University of California, Berkeley, California

ABSTRACT

Coarsening of the spinodal microstructure in copper-nickel-iron alloys has been studied in detail using transmission electron microscopy. Loss of coherency in this lamellar microstructure occurs by the capture of slip dislocations and subsequent multiplication at the interphase interfaces. Based on the observations, it is proposed that the multiplication process providing the misfit-accommodating dislocation loops proceeds by the spiraling of the captured dislocations around the platelets by climb, similarly to the formation of helical dislocations. Because the Burgers vector of the captured dislocation is inclined at 45° to the {100} interface, diffusion controlled rotation of the initial {100} coherent interface toward the {110} plane containing $\bar{b}$ occurs in order to lower the interfacial energy. This rotation of the semi-coherent interfaces results in a change of the initial platelet morphology to a microstructure containing rod-shaped and more equiaxed particles.

*Present address: Bell Laboratories, Murray Hill, N.J. 07974.

1. Introduction

The kinetics of spinodal decomposition in three Cu-Ni-Fe alloys and the corresponding microstructural changes as observed by electron metallography have been previously studied by Butler and Thomas[1] and by Livak and Thomas.[2] As the structure coarsens in these spinodal alloys, coherent platelets form on the {100} planes because this morphology minimizes the elastic strain energy of the two phase microstructure.[3] After long aging times at high temperatures, the coherent platelets lose coherency as interfacial dislocations form. In a Cu-Ni-Fe alloy of symmetrical composition (i.e. at the center of the miscibility gap), Butler and Thomas[1] observed that interfacial dislocations initially form when the platelet thickness is ~ 500Å and that loss of coherency occurs more rapidly at higher aging temperatures even though the lattice mismatch between the two fcc phases decreases with increasing temperature. Contrast experiments indicated that the most probable Burgers vectors of the interfacial dislocations are of the type a/2 ⟨110⟩ which are slip dislocations in these alloys. After very long aging times, networks of interfacial dislocations were observed and the semi-coherent interfaces were observed to rotate away from the {100} habit planes toward {110} planes. Subsequent electron metallography of semi-coherent particles in these Cu-Ni-Fe alloys demonstrated that the interfacial dislocations have a/2 ⟨110⟩ Burgers vectors that are inclined at 45° to the initially coherent {100} interfaces.[4]

The objective of the present study was to understand the mechanism for loss of coherency in spinodally decomposed and coarsened Cu-Ni-Fe alloys. Detailed analysis by transmission electron microscopy has led to a model for the development of the semi-coherent microstructures from the initially coherent platelet morphology which is consistent with observations. The relative energies of various types of interfacial structures have been considered and a dislocation mechanism is proposed to account for the generation of many misfit-accommodating dislocation loops from a single slip dislocation captured at the interface.

2. Experimental Procedures

2.1 Materials and Heat Treatment

The preparation of the alloys used in this study has been described earlier.[1,2] The compositions of the three alloys studied, in at.%, were:

alloy 1: 32.0 Cu - 45.5 Ni - 22.5 Fe;

alloy A: 51.5 Cu - 33.5 Ni - 15.0 Fe;

alloy 2: 64 Cu - 27 Ni - 9 Fe.

These alloy compositions lie along the same tie-line on the miscibility gap of the Cu-Ni-Fe system and the corresponding pseudo-binary phase diagram is given in Fig. 1 of reference 1. Samples for electron microscopy were prepared from eight mils thick sheet material that had been fabricated from the alloy ingots as described previously.[2]

Coupons of the three alloy compositions were solution treated at 1050°C for two hrs in evacuated quartz tubes and then quenched by breaking the tubes under ice water. Because the later stages of coarsening were to be studied, the quench rate was not critical to the subsequent aging treatments. Aging was done in evacuated quartz tubes at 775°C and 800°C for 50, 100 and 200 hrs.

2.2 Electron Microscopy

The heat treated coupons were thinned initially in a chemical polishing solution of 20 ml acetic acid, 10 ml nitric acid and 4 ml hydrochloric acid or on wet polishing paper to a thickness of 3-4 mils. Small discs were then spark cut from the coupons, polished on fine emery paper and electropolished in a double jet polisher using a chromic-acetic acid solution (75 gm CrO_3, 400 ml acetic acid and 12 ml water) kept at ~ 10°C. This polishing procedure worked fairly well even though the Cu rich phase polished preferentially.

The polished thin foils were examined in a Siemens Elmiskop IA electron microscope operated at 100 kV using a double tilt goniometer stage for contrast experiments. A few foils were examined in a Hitachi 650 kV electron microscope to study the interfacial dislocation arrays in thicker areas of the foils. In order to obtain a better understanding of the dislocation configurations, pairs of stereo micrographs were taken of some areas at 100 kV by tilting the foil 10-12° along a Kikuchi band so as to have the same diffraction conditions for both micrographs.

3. Observations

Most of the electron microscopy observations were made on alloy 2 which contains the largest volume fraction of the Cu rich phase in the three alloys studied. Since the Cu rich phase polished preferentially, it was easier to prepare good foils of alloy 2 than of the other two alloys. No interfacial dislocations were observed in specimens of the two asymmetrical alloys (compositions 1 and 2) aged at 700°C for 10, 40 and 200 hr and at 775°C for 10 hr. It was observed earlier[2] that the particles in these two alloys remained coherent after aging 1000 hr at 625°C. When aged at 800°C alloy 2 contains ~ 15% volume fraction of the Ni-Fe rich phase. This alloy remains single phase when aged at 825°C but the symmetrical alloy (composition A) is still inside the two phase region at this aging temperature.

Before coherency is lost, elongation of diffraction spots normal to the interfaces indicates that the two phases have constrained face centered tetragonal crystal structures with the c axes normal to the coherent interface and the two common a axes lying in the {100} interface. In samples aged at 625°C for 1000 hr, this spot elongation corresponds to a lattice parameter difference normal to the interface of $\Delta c = 1\%$.[5] In a sample of alloy 2 aged 200 hr at 775°C, the measured moiré fringe spacing corresponds to a constrained lattice misfit of 0.7% between the two coherent phases.

In many of the diffraction patterns taken of large coherent platelets, distinct streaks were observed lying along the <100> direction normal to

the interface. The length of these streaks, as shown in Fig. 1a, corresponds to a distance of 15-20Å in the crystal; and they probably are produced by the elastically strained region on either side of the coherent interface. In some cases two streaks separated by a small distance were observed to pass through the same spot, and this effect may be caused by a magnetic deflection due to the ferromagnetic Ni-Fe rich phase.

The microstructure prior to loss of coherency consists predominantly of thin platelets about 500Å thick and 1-2μ in length with {100} habit planes (see Fig. 2a). During the initial stages, loss of coherency does not occur throughout an entire grain but rather specific variants of the platelet morphology develop interfacial dislocations preferentially as shown in Fig. 2b. Furthermore different stages in the development of the dislocation arrays are often observed in adjacent particles. Another aspect of the selective nature of this process is that there appears to be no unique particle size but rather a range of particle thicknesses for which interfacial dislocations are observed. This is illustrated in Fig. 3 where two groups of four interfacial dislocations are seen at one platelet and all the surrounding platelets are still coherent.

As observed earlier by Butler and Thomas[1] and also in the present study, the semi-coherent interfaces develop more readily at higher temperatures for smaller platelet thicknesses and smaller lattice mismatch. Once the interfacial dislocations form, the semi-coherent particles grow more rapidly than the coherent platelets (e.g. Fig. 2b). As to the effect of volume fraction on the loss of coherency, the

symmetrical alloy containing an equal volume fraction of the two phases loses coherency sooner than the asymmetrical alloys aged at the same temperature. For example, Butler and Thomas observed some interfacial dislocations in foils of alloy A aged at 700°C for 40 hr whereas no interfacial dislocations were observed in foils of the asymmetrical alloys aged for 200 hr at the same temperature.

As the interfacial dislocations form, the interface changes its orientation towards a {110} plane. An example of this change is shown in the upper left corner of Fig. 2b where a few interfacial dislocations have formed. An even earlier stage of this process is shown in Fig. 3 where local rotation of the interface containing the dislocations has occurred. Figure 3 shows clearly that the "displacement" towards ⟨110⟩ is much larger than could be produced by each dislocation and therefore is not produced by slip alone as has been suggested earlier (4). Thus the change of orientation must be diffusion controlled, and occurs during the long aging times involved. As the interfacial dislocations develop further, the reorientation of the semi-coherent interface can result in a corrugated-shaped interface in which case the surfaces remain planar (see Fig. 4 in Ref. 4). However in other cases the interfaces become curved as they change orientation (e.g. Fig. 2b). Contrast analyses showed that the interfacial dislocations on the two surfaces of the corrugated-shaped interface have different Burgers vectors.[4]

Diffraction contrast experiments have shown that the Burgers vectors of the interfacial dislocations are of the type $\bar{b} = a/2\langle 110 \rangle$,

which is a slip dislocation in fcc crystals; and in most cases the Burgers vectors are inclined at 45° to the {100} coherent interfaces.[4] The dislocation lines generally lie along ⟨100⟩ directions in the interface although sometimes they are along ⟨110⟩ directions or take some intermediate orientation (see Fig. 4). Most of the observed semi-coherent interfaces contain one regular array of parrallel dislocations and in some cases a second set of dislocations which are more irregular in appearance. Sometimes the second set of dislocations is perpendicular to the first set and these dislocations often appear to be situated at steps on the interface as shown in Figure 5.

Stereo micrographs of the interfacial dislocations have revealed that some of the observed dislocations do not lie in the interface but rather extend into one of the phases.[5] Furthermore, high voltage electron microscopy has confirmed the observation of "stray" dislocations that do not lie in the interface (e.g. Fig. 6). Most of the micrographs show segments of interfacial dislocations that terminate at the foil surfaces. However, when the interfacial dislocations lie in the plane of the foil, it has been observed that these dislocations do in fact loop around the ends of the platelets.

An increase in the slip dislocation density accelerates the loss of coherency process as demonstrated by the following experiment. A sample of alloy 2 was aged at 800°C for 10 hr, reduced in thickness ~ 20% by cold rolling and then aged an additional 8 hr. Thin foils prepared from this deformed and aged specimen contained some particles that were beginning to lose coherency, whereas foils prepared from the

same material aged for 100 hr at 800°C but not deformed showed no evidence of loss of coherency.

4. Discussion

4.1 Semi-coherent Interfacial Structure and Energetics

A single interphase interface in this coherent platelet microstructure is similar to the interface between a thin metal film and the metal film substrate onto which it is evaporated. Various detailed theories of dislocation interphase boundaries in thin films have been developed; and Aaronson, et al.[6] have recently reviewed these theories including experimental observations for thin film and precipitate interphase boundaries. These theoretical results are used to explain the observations made on the loss of coherency in these Cu-Ni-Fe alloys.

The equilibrium crystal structures of the two phases are face-centered cubic with a small difference in lattice parameter. Just prior to loss of coherency the two phases have constrained face-centered tetragonal crystal structures with the two common a axes in the {100} interface and c axes normal to the interface. The Ni-Fe rich phase has $c_1 < \bar{a}$ whereas the Cu rich phase has $c_2 > \bar{a}$. The final semi-coherent microstructure of these spinodal alloys is expected to consist of spherical particles of the minor phase surrounded by a dislocation network containing three non-coplanar Burgers vectors that completely relieve the lattice mismatch along the three cube axes.

Based on geometrical considerations the most efficient misfit-accommodating dislocations are pure edge dislocations with the Burgers vector lying in the interface plane and the extra half plane of atoms extending into the phase with the smaller lattice parameter (i.e. the Ni-Fe rich phase). However, the observed interfacial dislocations in these Cu-Ni-Fe alloys have Burgers vectors inclined at 45° to the interface and are thus only partially effective in accommodating the lattice mismatch. Similar misfit-accommodating dislocations at {100} interphase boundaries have been observed by Matthews[7] and by Jesser and Matthews[8,9] in evaporated thin metal films. Based on the present results and also other reported observations of various interphase interfaces,[6,10] it is evident that the dislocations present at a semi-coherent interface are not necessarily the most efficient ones or those of minimum energy but rather may be those dislocations that are most easily generated or most readily available to relieve the coherency strains.

In explaining the loss of coherency in Cu-Ni-Fe alloys, it is useful to consider the relative changes in the interfacial energy for various interfacial structures. For this discussion the microstructure of interest is an array of parallel platelets that are initially coherent and that subsequently become semi-coherent (see Fig. 7). The interfacial energy consists of two parts: (1) a chemical component due to the difference in atomic bonding across the interface and (2) a structural component due to the elastic strain energy of the coherent interface or to the interfacial dislocation energy. The chemical compositions of the coherent platelets are given by the

coherent miscibility curve and thus are different from the compositions of the semi-coherent platelets. But since the lattice mismatch is small (1% or less), the difference in compositions between the coherent and semi-coherent particles is small and thus the chemical interfacial energies are about equal.

In order to estimate the structural interfacial energies for the coherent and semi-coherent states, the theoretical expressions derived by van der Merwe[11,12] for the interfacial energy of a thin film evaporated onto a substrate have been used. The details of the calculations are given in Appendix A where it is shown that the structural component of the coherent interfacial energy in these Cu-Ni-Fe alloys is ~ 330 ergs/cm^2. For the semi-coherent state, van der Merwe considered two simple cubic crystals in parallel orientation with the misfit in only one direction being accommodated by parallel edge dislocations. Using the equations resulting from van der Merwe's analysis, it is shown in Appendix A that the structural interfacial energy is ~ 250 ergs/cm^2 for a semi-coherent interface containing one set of dislocations with the Burgers vector inclined at 45° to the interface whereas this component of the energy is only ~ 225 ergs/cm^2 for a (110) interface with $\bar{b} = a/2\ [1\bar{1}0]$ lying in the interface. As the second set of interfacial dislocations is formed, the interfacial energy will be further reduced.

4.2 Proposed Mechanism for Loss of Coherency

Based on the experimental observations described previously, loss of coherency in this platelet microstructure occurs by the capture of

slip dislocations from the matrix with subsequent multiplication by climb of the dislocations at the interfaces to give the observed dislocation arrays. The punching of dislocation loops at or close to the particle - matrix interfaces is not expected to occur in these Cu-Ni-Fe alloys because of the small lattice mismatch ($< 1\%$). The calculations of Weatherly[13] indicate that the unconstrained transformation strain of a plate-shaped precipitate must be greater than 10% for loss of coherency to occur by punching. Also, a model for loss of coherency in modulated structures based on the prismatic punching mechanism[14] predicts that the maximum or critical modulation wavelength for loss of coherency decreases as the misfit increases. However, in these Cu-Ni-Fe alloys it is observed that loss of coherency occurs for smaller wavelengths at higher aging temperatures, where the misfit is less.

The proposed mechanism for loss of coherency involves a dislocation multiplication process in which a slip dislocation adsorbed at the interface spirals around the platelet to form interfacial dislocation loops. Resolution of the coherency stresses onto the various slip systems demonstrates a preferential stress interaction between a coherent {100} interface and a slip dislocation with its Burgers vector inclined at 45° to the interface. And the subsequent extension of the captured dislocation at the interface leads to the spiraling of the dislocation around the platelet. Weatherly and Nicholson[15] have observed a similar dislocation mechanism for the loss of coherency of rod shaped precipitates, and Matthews[16] has proposed a helical dislocation mechanism to explain the formation of misfit dislocation loops

around spherical particles.

Because loss of coherency occurs so slowly in these Cu-Ni-Fe alloys, it is assumed that the process is dependent on the availability of mobile dislocations already present in the crystal. It is possible that the slip dislocations are mostly generated at existing dislocation sources acted upon by the coherency stresses[4], since the matrix dislocation density is very low indeed prior to loss of coherency. However, sofar no detailed studies have been made to determine the origin of these dislocations. As an approximation to the actual coherency stress system, it is assumed that only the two normal stresses acting in the interface are non-zero for reasons discussed in appendix B. The results in Table I show that there is no preferential stress interaction between a coherent interface and a dislocation with its Burgers vector parallel to the interface. Consequently, only dislocations with Burgers vectors inclined at 45° to the {100} interfaces are attracted to the coherent interfaces. These are exactly the interfacial dislocations which we have observed. Whether a given dislocation is attracted or repelled by a coherent interface depends on the relative orientation of the phase with the smaller lattice parameter with respect to the extra half plane of atoms associated with the edge component of the dislocation. Also, since the orientation of the extra half plane of atoms depends on the sign of the Burgers vectors, dislocations of opposite sign will either be attracted or repelled from a given interface as shown in Table I.

The subsequent extension of the captured slip dislocation along the interface occurs as the platelet grows in thickness and the coherent strain energy increases (at a given aging temperature). Electron microscopy observations have shown that dislocation extension does occur at the platelet interfaces in these Cu-Ni-Fe alloys (e.g. Fig. 6). The physical situation is shown in Fig. 8a where a coherent platelet interface is intersected by a slip dislocation with its Burgers vector inclined at 45° to the interface. Jesser and Matthews[8] have discussed a similar situation for the extension of a dislocation along the interface between evaporated metal films. The elastic coherency stress at the interface causes the dislocation line to bow out in opposite directions in the two phases. As the platelet thickness increases, the bowed out segments take the form schematically shown in Fig. 8b, at which point the glide force acting on the dislocation becomes equal to the line tension of the misfit dislocation. With a further increase in the platelet thickness, the dislocation will extend by glide along the intersection of the slip plane with the interface as shown in Fig. 8c.

This stress activated extension of a dislocation at the interface is the first step in the proposed mechanism for loss of coherency which is shown in Fig. 9. In this example, a screw dislcoation with $\bar{b} = a/2\ [0\bar{1}1]$ extends by glide along [110] in the (001) interface which is the line of intersection of the $(\bar{1}11)$ slip plane and the (001) interface. But because the misfit directions are along ⟨100⟩ in the interface, the dislocation line will climb so that it lies along [100] in order to better accommodate the misfit. Since a stress acting on a

crystal is equivalent to a supersaturation of point defects, the coherency stresses provide a driving force for dislocation climb which can occur rapidly at these high aging temperatures (800°C $\simeq$ 0.75 T_m). The initiation of this process depends on the availability of suitable slip dislocations; and the overall process is both thermally and stress activated occurring at some critical combination of temperature and platelet thickness which is consistent with the observations that loss of coherency occurs more rapidly at higher temperatures and begins for smaller platelet thicknesses at higher temperatures.

The continued development of the spiral dislocation around the platelet is in some ways analogous to the formation and growth of helical dislocations, by climbing screws as observed by Thomas & Whelan.[17] The equilibrium form of a dislocation acted upon by an external mechanical or chemical force is either a straight line or a helix. The coherency stresses acting on the extended dislocation shown in Fig. 9c provide a driving force for the climb of the dislocation into a spiral around the platelet interface that relieves the elastic coherency strains. Obviously the climb rate will increase with increasing aging temperature because of the diffusion involved. Thus the capture and climb of dislocations are additive to the overall process of loss of coherency. The micrograph of Fig. 6 is in agreement with this idea.

The two equilibrium phases differ in lattice parameters, consequently a net flux of atoms must diffuse from the Cu rich phase, with the larger lattice parameter, to the Cu poor phase so as to maintain

the correct correspondence of atomic planes across the semi-coherent interface.

As the dislocation spirals around the platelet, closed loops will be formed from each turn of the spiral as shown in Fig. 9d. Opposite sides of each turn are attracted to each other since the dislocation line changes its sense of direction as it winds around the platelet. As the first turn of the spiral forms a loop, successive turns of the spiral will be in various stages of formation so that many dislocation loops can be generated from a single slip dislocation captured at the interface. Other sets of interfacial dislocations with different Burgers vectors can be produced by this same dislocation mechanism. However, the subsequent dislocations will interact with the initial set of dislocations and will thus be hindered in climbing around the particle (e.g. Fig. 6 in Ref. 4).

4.3 Change in Particle Morphology

The rotation of the semi-coherent interface toward a {110} orientation can now be understood in terms of the proposed model for loss of coherency. Slip dislocations with Burgers vectors inclined at 45° to the {100} coherent interfaces are preferentially attracted to the interfaces as shown by the resolution of the coherency stresses. The driving force for the rotation of a semi-coherent interface toward a {110} orientation is the difference in structural interfacial energies between a {100} semi-coherent interface with $\bar{b}$ at 45° to it and a {110} interface which contains $\bar{b}$. The local rotation of the interface plane at interfacial dislocations is evident in Fig. 3. The

necessary changes in composition during this rotation occur by diffusion as evidence by the observed rates.

As the semi-coherent interfaces rotate, the initially coherent {100} platelets become semi-coherent rods with faces parallel to {110} planes and the rod axes along ⟨100⟩ as shown in Fig. 4 of Ref. 4. Many semi-coherent particles are observed that only have interfacial dislocations in parallel interfaces which have rotated away from the initial {100} orientation (see Fig. 2b). This observation is consistent with the proposed model of a spiral dislocation around the platelet and the subsequent rotation of the semi-coherent interfaces.

5. Summary

The transmission electron microscopy observations have revealed some unusual effects associated with the loss of coherency in spinodally decomposed Cu-Ni-Fe alloys. Slip dislocations with their Burgers vectors inclined at 45° to the initially coherent {100} interfaces are observed, even though such dislocations are only partly effective in accommodating the misfit at the interfaces. Unusual dislocation configurations are observed with some dislocation lines extending into one of the phases, suggestive of a complex climb mechanism. Also, the process occurs preferentially at a few platelets while the other platelets in the same grain remain coherent. As coherency is being lost, the initial {100} interface is observed to rotate toward a {110} plane.

The proposed mechanism for the spiraling of a captured slip dislocation around the coherent platelet is able to explain these

observations. The operation of this mechanism is dependent on the availability of suitable slip dislocations present in the crystal and occurs by a rather complex climb process that is thermally and stress activated. The rotation of the interface is related to the observation that the Burgers vectors of the interfacial dislocations are inclined at 45° to the {100} interfaces. The proposed dislocation mechanism for loss of coherency is consistent with experimental observations made on other alloys as reported in the literature.

Acknowledgments

We wish to thank the United States Atomic Energy Commission through the Inorganic Materials Research Division of the Lawrence Berkeley Laboratory for financial support of this research. This work was done in partial fulfillment of the Ph.D. requirements by one of the authors (RJL) who also acknowledges support of a National Science Foundation Graduate Fellowship.

Appendix A

Calculation of Structural Interfacial Energies

Theoretical expressions derived for the structural component of the interfacial energy in an epitaxial evaporated thin film will be used to estimate the structural interfacial energies of various platelet interfaces.

However, the analysis for the case of thin films only approximates the platelet case since the thin film is not elastically constrained at its free surface. In the following discussion, the film thickness (h) will be assumed to be equivalent to one-half of the platelet thickness.

Van der Merwe[11,12] has considered the case of two simple cubic crystals in parallel orientation that differ in lattice parameter along only one cube axis. If the film thickness (h) and the misfit ($\delta = (a_1 - a_2)/1/2(a_1 + a_2)$) are sufficiently small, then a fully coherent boundary will have a lower energy than a semi-coherent one with the equilibrium configuration of misfit dislocations. The elastic energy required to homogeneously deform the thin film in one direction is[12]

$$E_{struct}^{coherent} = \frac{\mu_1(1 - \nu_1)h\delta'^2}{1 - 2\nu_1} \qquad (1)$$

For the case of Cu-Ni-Fe, $\delta' = (a_1 - a_2)/a_1 \simeq \delta$ at small values, and a_1 and a_2 are the lattice parameters of the two phases, the one having lower shear modulus μ_1 and Poisson's ratio ν_1 As a first approximation,

this elastic strain energy is doubled if the film is homogeneously deformed in two directions. Because Eq. (1) is for the case where all the elastic strain energy is accommodated in the thin film, it gives too large an energy for the case where both crystals are deformed elastically to accommodate the misfit.

For the semi-coherent interface, van der Merwe has considered two simple cubic crystals in parallel orientation with the misfit in only one direction being accommodated by parallel edge dislocations. By treating the interaction across the boundary with a sinusoidal force law and the interaction within a given crystal on the basis of an elastic continuum, the following expression was obtained for the structural interfacial energy of two semi-infinite crystals:[11]

$$E_{struct}^{semi\text{-}coh} = \frac{\mu c}{4\pi^2}\{1 + \beta - (1+\beta^2)^{1/2} + \beta \ln[2\beta(1+\beta^2)^{1/2} - 2\beta^2]\} \qquad (2)$$

where

$$\beta = 2\pi\delta(\Omega/\mu)$$

and

$$\frac{1}{\Omega} = [(1 - \nu_1)/\mu_1] + [(1 - \nu_2)/\mu_2]$$

In these equations $c = 1/2(a_1 + a_2)$, μ = shear modulus at the boundary, μ_1 and μ_2 = the shear moduli within phases 1 and 2 respectively, and ν_1 and ν_2 = Poisson's ratio within 1 and 2. In a subsequent paper van der Merwe[12] showed that the interfacial energy for a film of "infinite" thickness is very nearly the same as for a film of finite thickness greater than one-half the separation of the misfit dislocations. This

approximation is reasonable for the sizes of phases considered in this paper.

Loss of coherency occurs for the critical value of misfit, δ_c', at which $E_{struct}^{coherent} = E_{struct}^{semi\text{-}coh}$. Assuming that the critical misfit is sufficiently small so that $\beta^2 \simeq 0$ and that $\nu_1 = \nu_2 = 1/3$, and $\mu_1 = \mu_2 = \mu$, the critical thickness of the overgrowth corresponding to δ_c' is[6]

$$h_c = \frac{3a_1[1 - \ln(3\pi\delta_c')]}{16\pi\delta_c'} \qquad (3)$$

This equation can be used to estimate the critical thickness of a coherent platelet ($2h_c$) at which misfit dislocations lower the structural interfacial energy.

The above equations resulting from van der Merwe's analysis will be used to estimate the energies of various interfacial structures in the Cu-Ni-Fe alloys. The misfit parameter for these alloys aged at 775°C is $\delta \simeq 0.8\%$ normal to the interface as coherency is being lost as measured from Moiré fringes[5] and from split diffraction spots.[1] This value is probably representative of the equilibrium misfit parameter (i.e. the unconstrained misfit) for the semi-coherent particle because of the stress relaxation normal to the platelet interface. Using this value of $\delta = 0.8\%$ and $a_1 \simeq \bar{a} = 3.59$Å, the critical thickness of the platelets for loss of coherency is found from Eq. (3) to be $2h_c \simeq 200$Å.

In order to calculate the structural interfacial energy for the coherent interface, an appropriate thickness of the platelet must be used. An upper limit for this energy is given by taking h = 250Å which is one-half of the observed thickness of the coherent platelets, and a lower limit is given by using the above calculated critical thickness for loss of coherency (i.e. h = 100Å). Taking $\mu_1 \simeq \bar{\mu} = 7.3\times10^{11}$ dyn/cm^2. (assuming $\mu \propto$ composition), $\nu_1 = 1/3$, $\delta' = 0.8\%$ and using these two values for h, the coherent structural energy for misfit along one direction is found from Eq. (1) to be $E_{struct}^{coherent} = 95\text{-}235$ ergs/cm^2 with a mean value of 165 ergs/cm^2. For misfit along two cube directions the total structural interfacial energy is ~ 330 ergs/cm^2.

For the semi-coherent interface, two cases will be considered: (1) a (100) interface with the Burgers vector $\bar{b} = a/2[1\bar{1}0]$ inclined at 45° to the interface and the dislocation line along [001]; and (2) a (110) interface with $\bar{b} = a/2\ [1\bar{1}0]$ lying in the interface and the dislocation line along [001]. The following values of the parameters will be used for the calculations.

$$c = 1/2(a_1 + a_2) = 3.59\text{Å}$$

$$\delta = 0.8\%$$

$$\nu_1 = \nu_2 = 1/3$$

$$\mu_1 = 8.3\times10^{11} \text{ dyn/cm}^2$$

$$\mu_2 = 6.3\times10^{11} \text{ dyn/cm}^2$$

$$\mu = 1/2(u_1 + u_2) = 7.3\times10^{11} \text{ dyn/cm}^2$$

$$\Omega = 5.4\times10^{11} \text{ dyn/cm}^2$$

$$\beta = 3.7\times10^{-2}$$

The values for the shear modulus are estimated from the values of the individual components, extrapolated assuming linear composition dependence. (e.g. Ref. 1). As an approximation, it is assumed that $\mu \propto$ composition. Substituting these values into Eq. (2), one calculates for the (100) interface that $E_{struct}^{semi-coh} = 85$ ergs/cm^2. This value underestimates the actual energy because the equation derived by van der Merwe is for the case of parallel pure edge dislocations with Burgers vector equal to the lattice parameter whereas the observed interfacial dislocations have a resolved edge component lying in the interface equal to one-half the lattice parameter. Consequently, a greater number of these inefficient dislocations are required to completely accommodate the misfit at the interface. If only one set of dislocations is present at the interface, then the misfit in the orthogonal cube direction is still accommodated by elastic strain and the total structural interfacial energy for this case is $E_{struct}^{semi-coh}$ (100) $\simeq$ 85 ergs/cm^2 + 165 ergs/cm^2 = 250 ergs/cm^2.

For the second type of semi-coherent interface parallel to (110), a lower density of misfit dislocations is required compared to the (100) interface since the Burgers vector lies in the interface and the dislocations are pure edge in character. Thus, the structural interfacial energy of the (110) interface will be less than that of the (100) interface. This difference between the two interfaces also follows from Eq. (2) used to calculate the semi-coherent interfacial energy. The reference lattice parameter, c, in this equation corresponds to the atomic distance along the misfit direction. For the (110)

interface this misfit direction is $[1\bar{1}0]$ with $a_{\langle 110 \rangle} = |\bar{b}| = 2.54\text{Å}$. Using this value of c in Eq. (2), one obtains $E^{\text{semi-coh}}_{\text{struct}}(110) = 60\ \text{ergs/cm}^2$; and if only one set of dislocations is present at the interface, then the total structural interfacial energy for this case is $E^{\text{semi-coh}}_{\text{struct}}(110) \simeq 225\ \text{ergs/cm}^2$. As more interfacial dislocations with other Burgers vectors to accommodate the misfit develop at the interface, the structural interfacial energy will be reduced further.

Appendix B

Resolution of Coherency Stresses Acting on Glide Dislocations

The following discussion and stress analysis are based on an analysis done by Dahlgren[18] for the calculated yield stress of a coherent platelet microstructure. As an approximation to the coherency stresses acting on the platelets, it will be assumed that the stress normal to the interface is zero, $\sigma_{zz} = 0$ (see Fig. 7), since the total displacement across many platelets is small and that the two stresses parallel to the interface are equal, $\sigma_{xx} = \sigma_{yy}$, since the two phases are tetragonal. Because the four-fold symmetry axis of the tetragonal structure is taken normal to the x-y plane, $\sigma_{xy} = 0$. The other two shear stresses, σ_{yz} and σ_{xz}, are not zero, but for thin platelets these stresses are small. If the platelet thickness is much less than its length, then these shear stresses can be neglected.

For an isotropic material

$$\varepsilon_{xx} = \frac{1}{E} \{\sigma_{xx} - \nu(\sigma_{yy} + \sigma_{zz})\}$$

where E is Young's modulus and ν is Poisson's ratio. Since it is being assumed that $\sigma_{xx} = \sigma_{yy}$ and $\sigma_{zz} = 0$ this equation gives

$$\varepsilon_{xx} = \frac{1}{E} (\sigma_{xx} - \nu\sigma_{xx})$$

and

$$\sigma_{xx} = \frac{E}{1-\nu} \varepsilon_{xx}$$

where the coherency strain is $\varepsilon_{xx} = (\bar{a} - a_{io})/a_{io}$, $\bar{a}$ being the common non-equilibrium lattice parameter ($\bar{a} \simeq 1/2(a_{1o} + a_{2o})$) and a_{io} being the appropriate equilibrium cubic lattice parameter of the i^{th} phase. This elastic coherency strain has a smaller value than the previously defined misfit strain, $\delta' = (a_1 - a_2)/a_1$, for the equilibrium misfit dislocation structure; and as an approximation $\varepsilon_{xx} \simeq 1/2\ \delta = 0.4\%$ for these Cu-Ni-Fe alloys. Taking $\nu = 1/3$, $E = 2\times10^4$ kg/mm^2 and $\varepsilon_{xx} = 0.004$, the corresponding value of the coherency stress is

$$\sigma_{xx} = \sigma_{yy} \simeq 120 \text{ kg/mm}^2$$

The Ni-Fe rich phase, with a smaller equilibrium lattice parameter, is acted on by a tensile stress and the Cu rich phase by a compressive stress.

The interaction between the coherency stresses and the slip dislocations is found by resolving the shear components of these stresses on the slip plane and in the slip direction. For fcc crystals the slip planes are {111} and the slip directions are ⟨110⟩. The stress resolution can be done using the stress tensor and the following formula:

$$\sigma_{\mu\rho} = \sum_{i,j} \sigma_{ij}\, l_{i\mu}\, l_{j\rho}$$

where $\sigma_{\mu\rho}$ is the resolved stress acting in the ρ direction on the slip plane with normal μ and $l_{i\mu}$ and $l_{j\mu}$ are direction cosines between the given directions. Table 1 gives these resolved shear stresses

for the case of a (001) interface and all possible Burgers vectors. The normals to the slip planes all point in the positive z direction to give consistent results.

References

1. E. P. Butler and G. Thomas, Acta Met. 18, 347 (1970).
2. R. J. Livak and G. Thomas, Acta Met. 19, 497 (1971).
3. A. G. Khachaturyan, Phys. Status Solidi. 35, 119 (1969).
4. M. Bouchard, R. J. Livak and G. Thomas, Surface Science 31, 275 (1972).
5. R. J. Livak, Ph.D. Thesis, University of California, Berkeley, LBL-1107, Sept. 1972.
6. H. I. Aaronson, C. Laird and K. R. Kinsman, in Phase Transformations, p. 339. Amer. Soc. for Metals (1970).
7. J. W. Matthews, Phil. Mag. 13, 1207 (1966).
8. W. A. Jesser and J. W. Matthews, Phil. Mag. 15, 1097 (1967).
9. W. A. Jesser and J. W. Matthews, Phil. Mag. 17, 595 (1968).
10. K. R. Kinsman and H. I. Aaronson, "Structure of Crystalline Interfaces" Theory of Microstructure, Ed. J. L. McCan, International Microstructure Analysis Society, Denver, Colorado (1972).
11. J. H. van der Merwe, J. Appl. Phys. 34, 117 (1963).
12. J. H. van der Merwe, ibid., 123.
13. G. C. Weatherly, Phil. Mag. 17, 791 (1968).
14. D. de Fontaine, Acta Met. 17, 477 (1969).
15. G. C. Weatherly and R. B. Nicholson, Phil. Mag. 17, 801 (1968).
16. J. W. Matthews, Scripta Met. 5, 1056 (1971).
17. G. Thomas and M. J. Whelan, Phil. Mag., 4, 511, (1969).
18. S. D. Dahlgren, Ph.D. Thesis, University of California, Berkeley, UCRL-16846, May 1966.

Table 1. Stress interaction between (001) coherent interface and Burgers vectors of slip dislocations.

Burgers Vector	Slip Plane	Resolved Shear Stress
$\pm[110]$	$(\bar{1}11)$ $(1\bar{1}1)$	0
$\pm[\bar{1}10]$	(111) $(\bar{1}\bar{1}1)$	0
$[101]$	$(\bar{1}11)$ $(\bar{1}\bar{1}1)$	$-\sigma_r$
$[\bar{1}0\bar{1}]$	$(\bar{1}11)$ $(\bar{1}\bar{1}1)$	$+\sigma_r$
$[\bar{1}01]$	(111) $(1\bar{1}1)$	$-\sigma_r$
$[10\bar{1}]$	(111) $(1\bar{1}1)$	$+\sigma_r$
$[011]$	$(1\bar{1}1)$ $(\bar{1}\bar{1}1)$	$-\sigma_r$
$[0\bar{1}\bar{1}]$	$(1\bar{1}1)$ $(\bar{1}\bar{1}1)$	$+\sigma_r$
$[0\bar{1}1]$	(111) $(\bar{1}11)$	$-\sigma_r$
$[01\bar{1}]$	(111) $(\bar{1}11)$	$+\sigma_r$

$$\sigma_r = \sigma_{xx}/\sqrt{6} = 50 \text{ kg/mm}^2$$

The plus (+) means attraction and the minus (-) means repulsion for the interface of the phase under a tensile stress (i.e. the Ni-Fe rich phase with $c_1 < \bar{a}$).

Figure Captions

Fig. 1. Electron diffraction pattern (a) and corresponding bright field image (b) showing split streaks at the $51\bar{1}$ reflection that are normal to coherent platelets in alloy 2 aged 100 hrs at 800°C.

Fig. 2. (a) Transmission electron micrograph showing coherent platelets about 500Å thick and 1-2 μm long in a foil of alloy 2 aged 100 hrs at 800°C. (b) Micrograph taken of the same grain showing some particles losing coherency. Note rotation of semi-coherent interface in the upper left corner. Electron beam parallel to [011] zone axis.

Fig. 3. Bright field micrograph of alloy 2 aged 100 hrs at 800°C showing a dislocation configuration suggestive of a spiraling mechanism for the formation of interfacial dislocations. Note local rotation of interface at dislocation lines.

Fig. 4. Bright field micrograph of alloy 2 aged 100 hrs at 800°C showing some interfacial dislocations that do not lie along ⟨001⟩ (see arrows). Also note the unequal number of dislocations at the two interfaces.

Fig. 5. Bright field micrographs of the same area under different diffraction conditions of the symmetrical alloy aged 100 hrs at 775°C showing dislocations visible in (b) that lie at steps on the interfaces visible in (a). When (a) is viewed in stereo the steps are evident.

Fig. 6. High voltage (650 keV) electron micrograph of alloy 2 aged 100 hrs at 800°C showing a dislocation being extended along the interface and looping back upon itself (see arrow).

Fig. 7. Schematic drawing of coherent platelet microstructure used in calculating the interfacial energies and also for the resolution of the coherency stresses on the various slip systems.

Fig. 8. Plane section through the platelet microstructure parallel to the $(\bar{1}11)$ slip plane showing the stress activated extension of a slip dislocation along the coherent interface.

Fig. 9. Proposed mechanism for the spiraling of a captured slip dislocation around a coherent platelet to form misfit-accommodating dislocation loops. Refer to δ 4.2 for discussion.

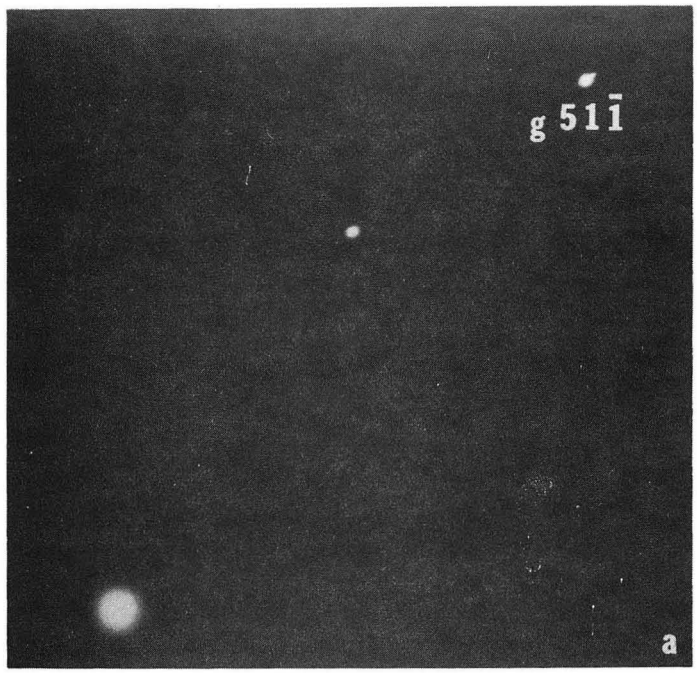

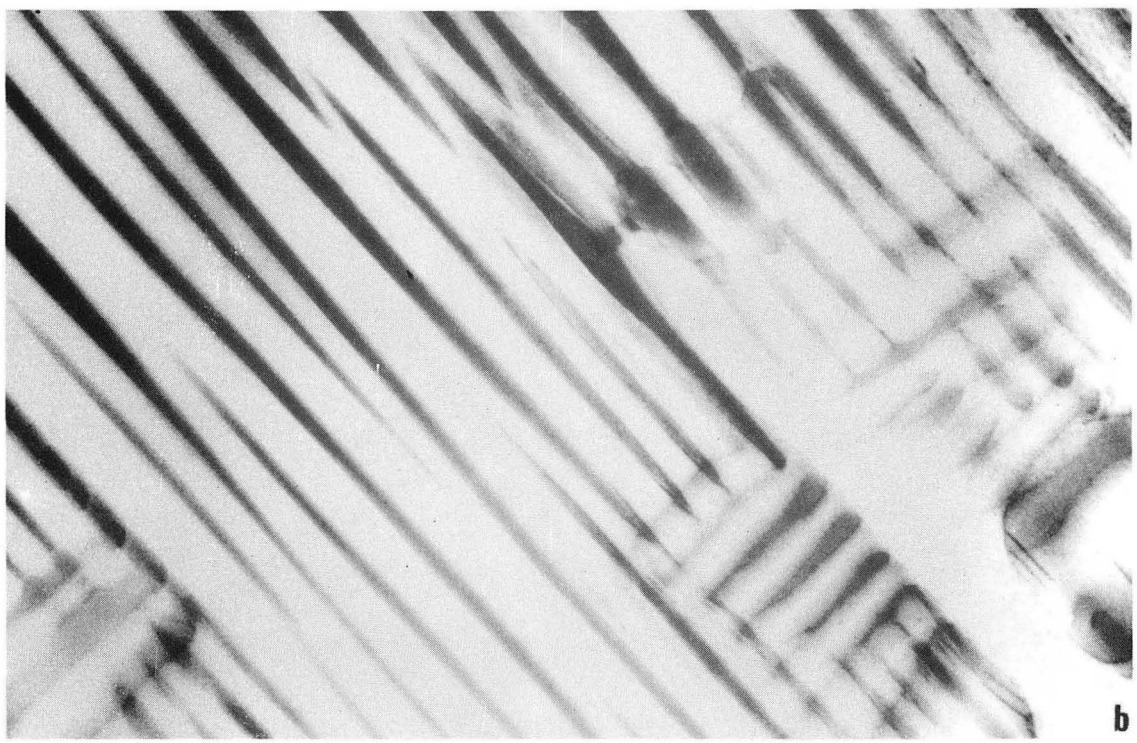

XBB 729-4745

Fig. 1

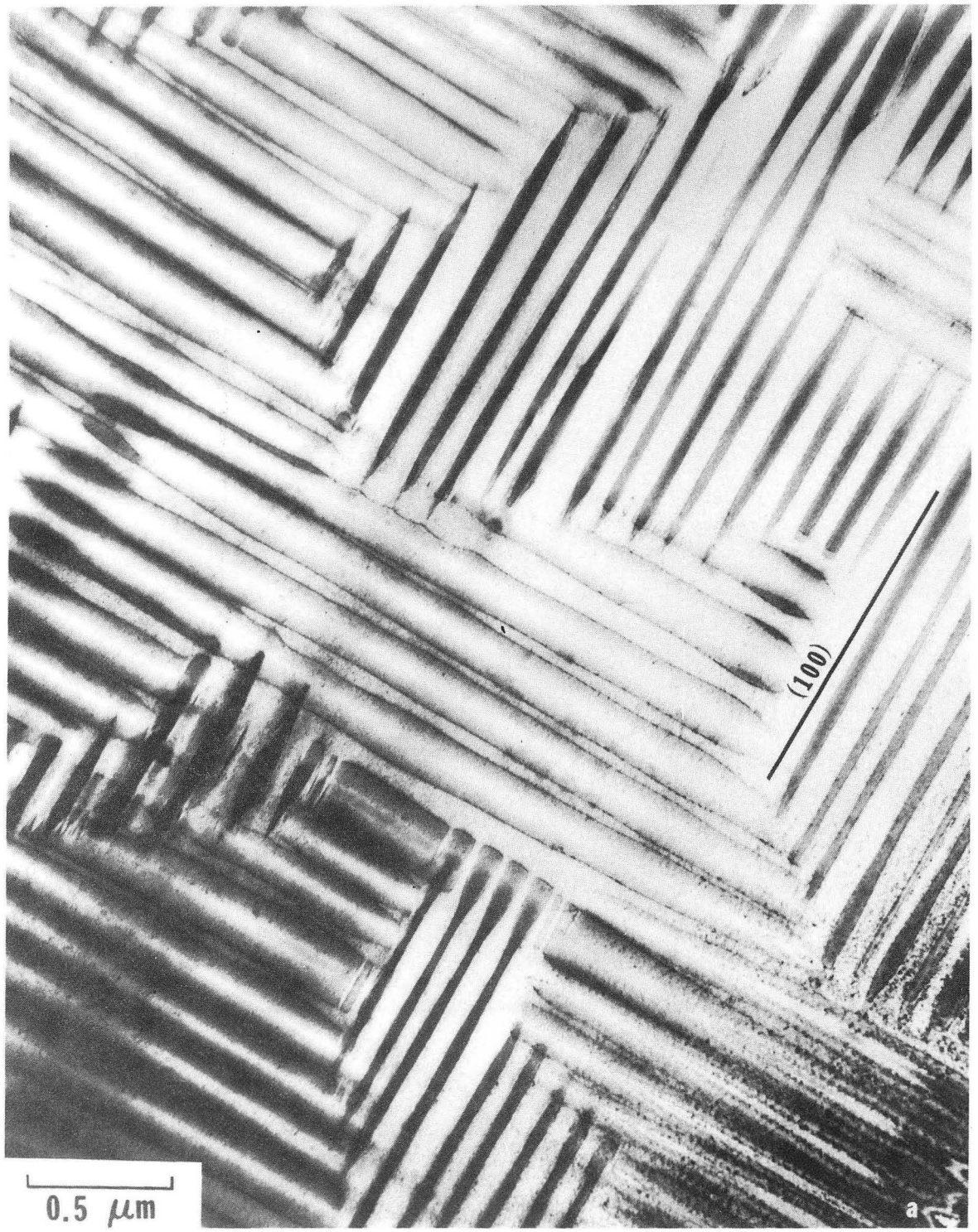

XBB 729-4744

Fig. 2a

XBB 729-4742

Fig. 2b

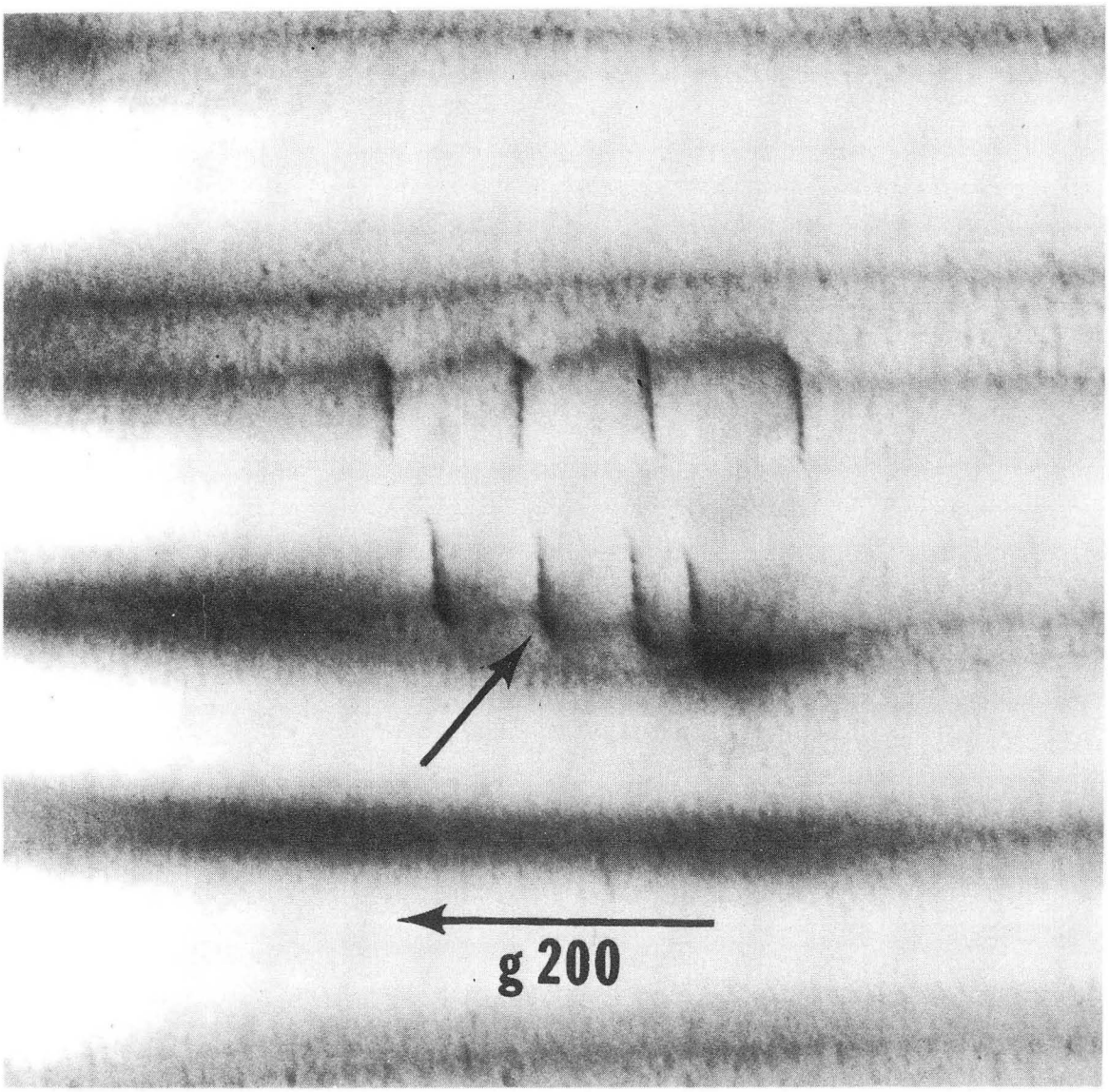

XBB 729-4726

Fig. 3

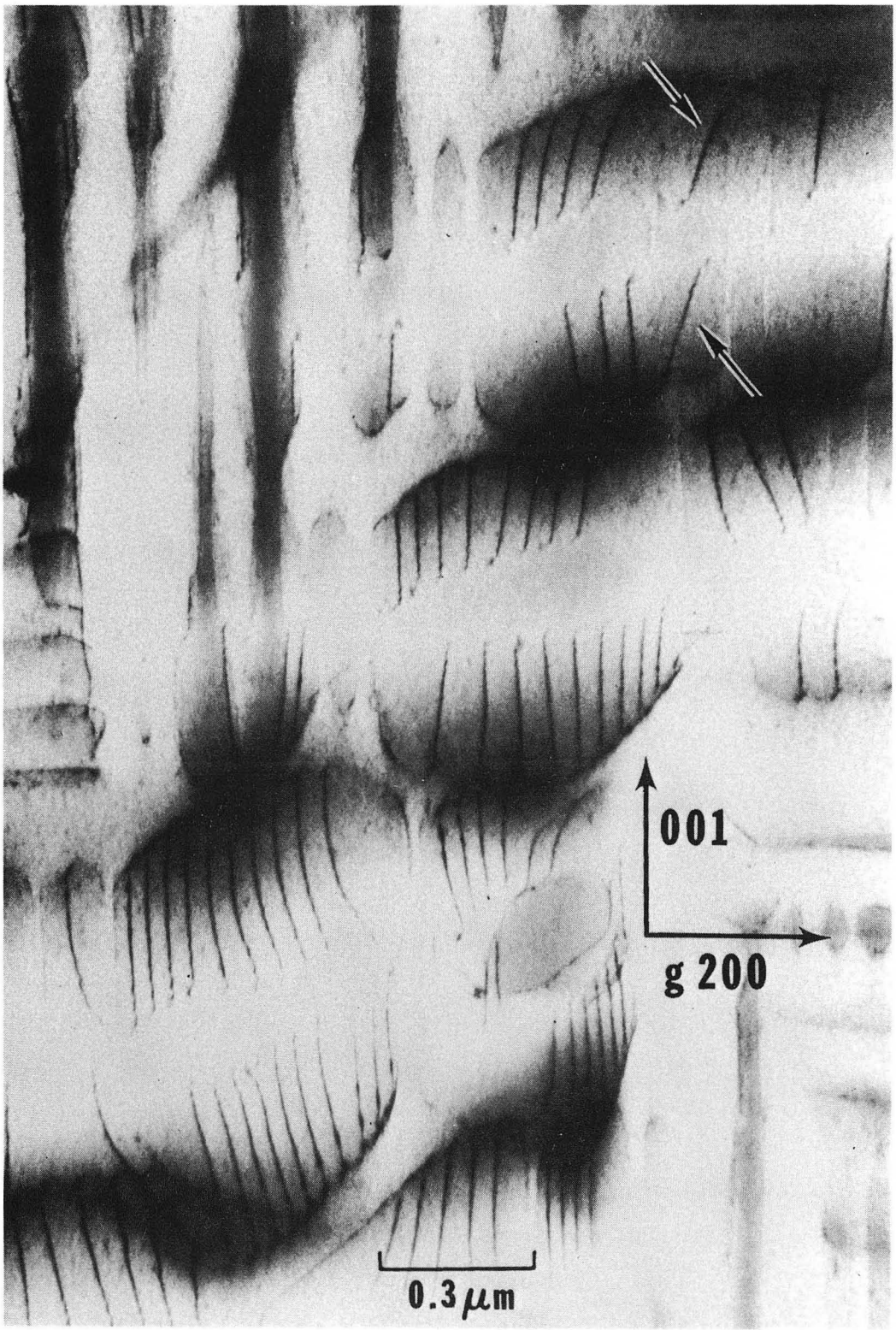

XBB 729-4730

Fig. 4

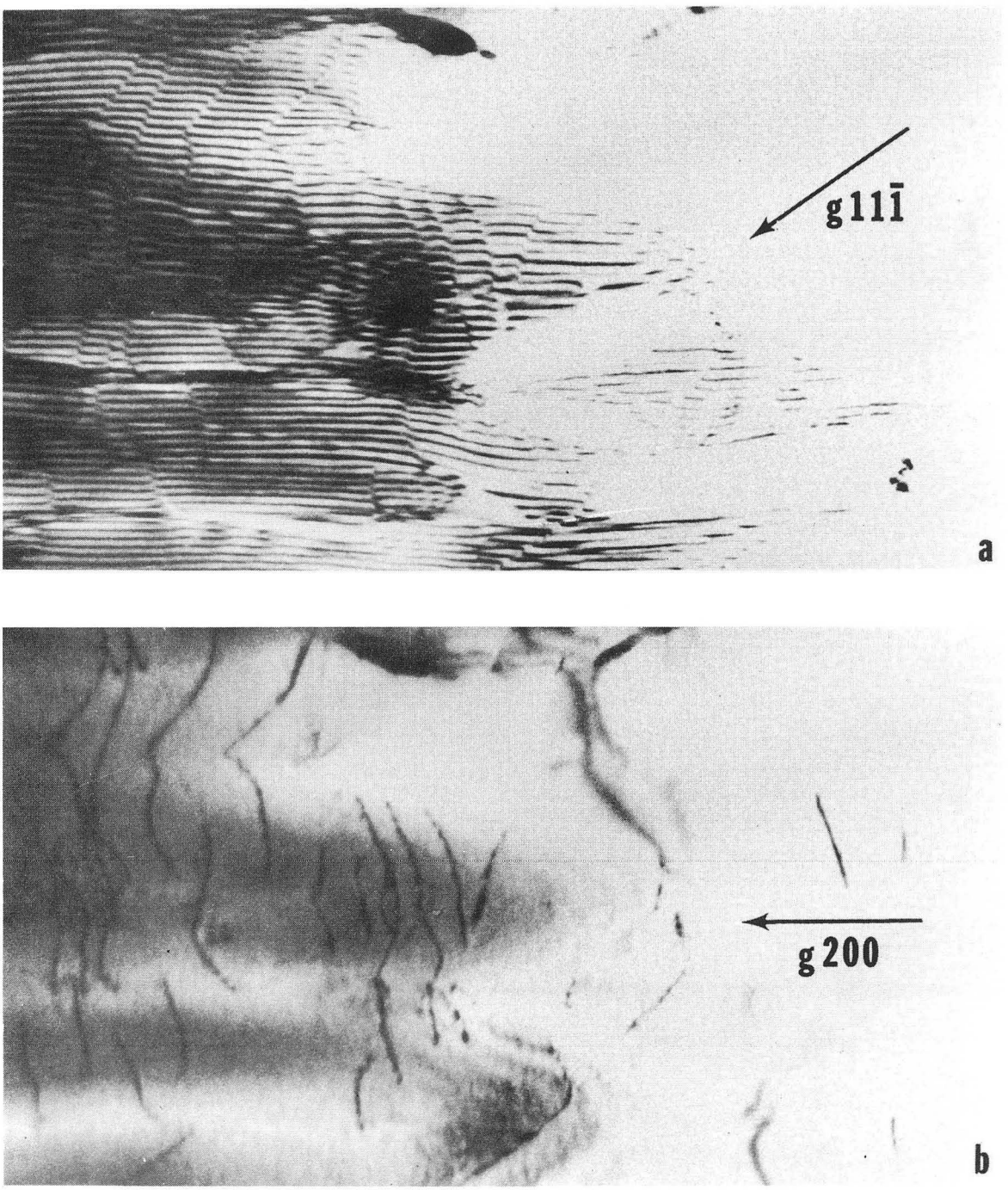

XBB 729-4728

Fig. 5

XBB 729-4736

Fig. 6

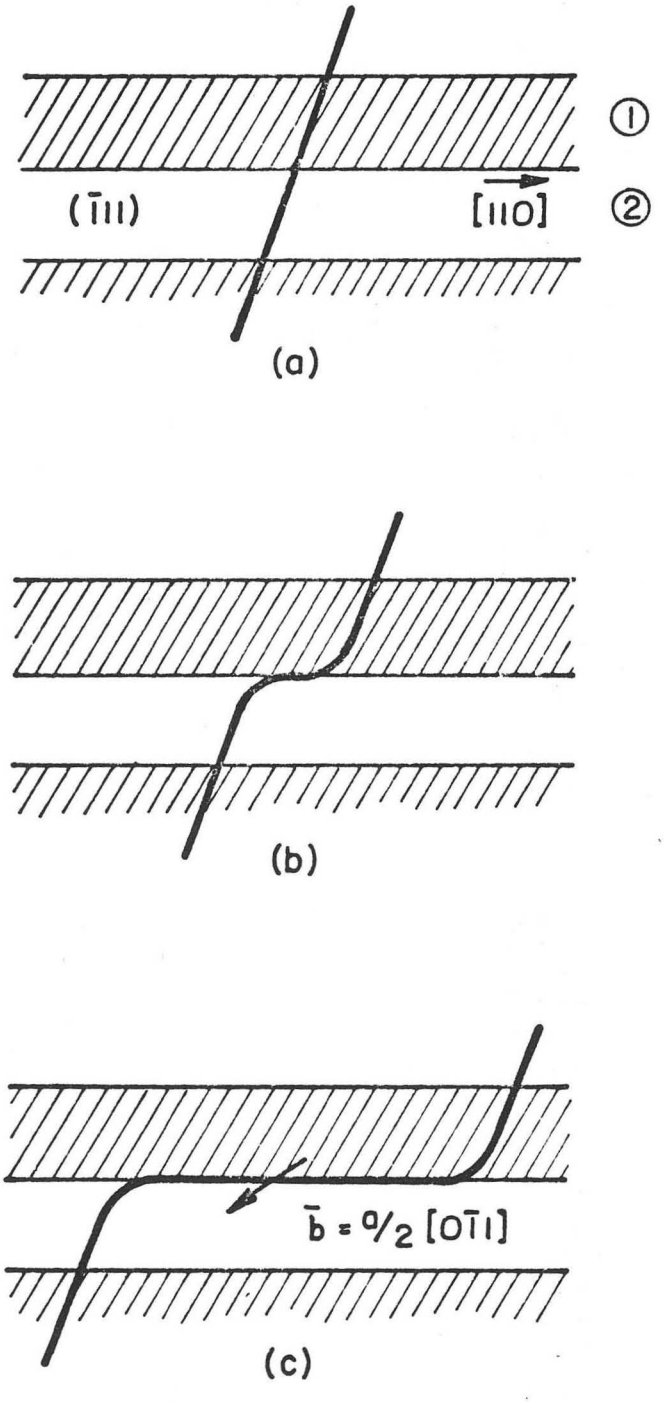

XBL 729-6903

Fig. 7

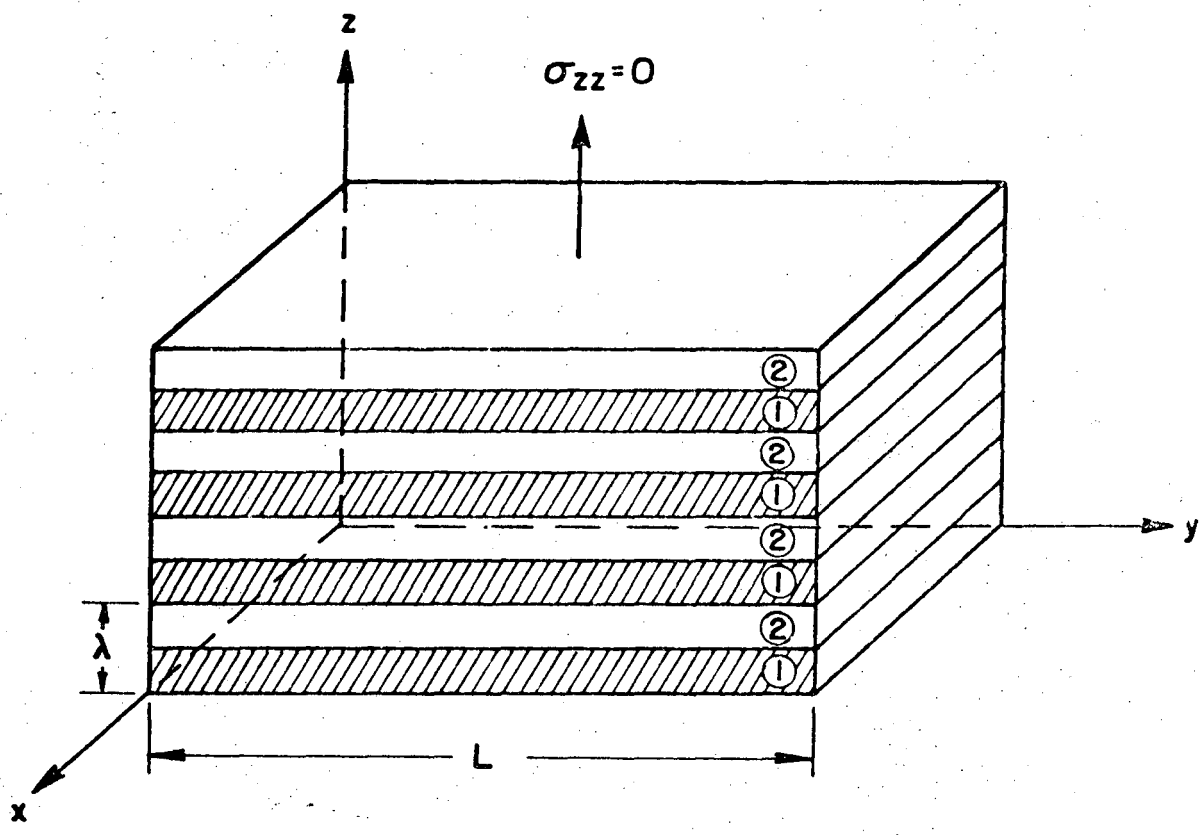

XBL729-6901

Fig. 8

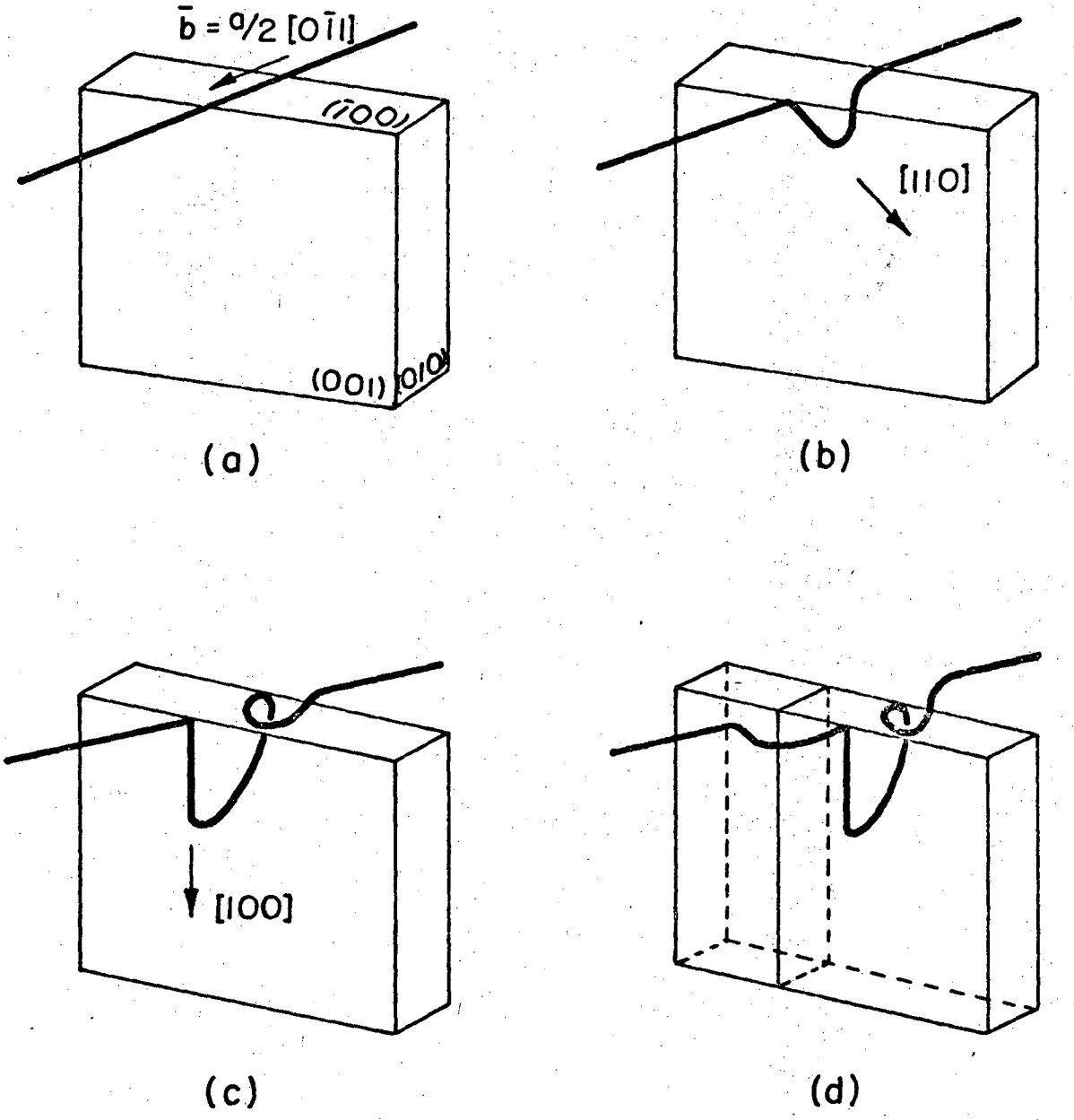

Fig. 9

TECHNICAL INFORMATION DIVISION
LAWRENCE BERKELEY LABORATORY
UNIVERSITY OF CALIFORNIA
BERKELEY, CALIFORNIA 94720